# Reactions of Charged Substrates. 2. Gas-Phase Dissociation of 2′-Substituted Nicotinamide Arabinosides

Neil Buckley,* Anthony L. Handlon,† David Maltby, Alma L. Burlingame, and Norman J. Oppenheimer*

*The Department of Pharmaceutical Chemistry, S-926, Box 0446, The University of California, San Francisco, California 94143-0446*

*Received August 13, 1993 (Revised Manuscript Received March 10, 1994®)*

The relative abundances of ribosyl oxocarbenium ion-related cations in the gas-phase dissociation of five 2′-substituted β-nicotinamide arabinosides (substituents = H, OH, $NH_2$, NAc, F) follow the Taft equation with $\sigma_F$. The first-order rate constants for the pH-independent hydrolysis of these substrates follow $\varrho_I$, which is based on solution acidities of the same series of compounds used to define $\sigma_F$ in the gas phase. The value of $\varrho$ is much greater in solution ($\varrho_I = -6.7$) than in the gas phase ($\varrho_F = -0.75$). There is direct evidence that the NAc substrate reacts through an ion–dipole complex. Energy profiles were calculated in AM1; while there are some apparent anomalies in the method that can be sorted out easily, the activation enthalpies and energies of the various structures are consistent with the proposed mechanism. A plot of the AM1-calculated values of $\Delta H^{\ddagger}$ for gas-phase dissociation vs the log of the relative abundances for the respective species is linear, as is a plot of the solution $\Delta G^{\ddagger}$ and the gas-phase $\Delta H^{\ddagger}$. Comparison of solution and gas-phase results suggests that an ion–dipole complex is an intermediate in both phases, but that the rate-limiting step is different.

## Introduction

A part of continuing model studies for the hydrolysis of nicotinamide adenine dinucleotide ($NAD^+$),[1] Handlon and Oppenheimer[2] recently reported rate constants for the pH-independent hydrolysis of a series of 2′-substituted β-nicotinamide arabinosides (**1a–e**) with different oxocarbenium ion intermediates; kinetics and a Taft correlation are consistent with a dissociative mechanism. Studies by Schuber and his colleagues[3] of the uncatalyzed and $NAD^+$ glycohydrolase [EC 3.2.2.5]-catalyzed hydrolysis of $NAD^+$ analogues with substituted pyridines as leaving groups also supports this mechanism. Recent results for the enzyme-catalyzed dissociation of 2′-substituted $NAD^+$ analogs reproduce almost exactly the slope of the Taft plot found for nonenzymatic hydrolysis of the arabino and ribo derivatives.[4]

For comparison with these solution results, we have measured the gas-phase dissociation of **1a–e** using tandem positive-ion liquid secondary ion mass spectrometry (LSIMS). With these techniques, it is possible to study directly the gas-phase dissociation of positively charged substrates without the relatively harsh conditions needed to produce the molecular ion in chemical ionization or electron impact methods. Nontandem spectra give reasonable correlations for these substrates, but the tandem correlations are measurably better because only the molecular ion is collisionally activated and dissociates in MSII. The experimental results and the energies and structures obtained with AM1 suggest that gas-phase dissociation of **1a–e** occurs through an ion–dipole complex (IDC) intermediate.

## Experimental Section

**Experimental.** Syntheses of the substrates have been reported.[5] Tandem mass spectra were recorded under identical conditions in the positive ion mode on a 4-sector Kratos Concept II HH mass spectrometer fitted with an optically coupled 4% diode array detector on MS II. Substrates were sputtered from a glycerol matrix with $Cs^+$ (18 keV), and the molecular ion was sorted into MSII where fragmentation was induced by collisional activation with helium. Results are the averages of several runs (<5% error); nontandem LSIMS spectra give the same trends, although the precision is not as good.

**Computational Methods.** Calculations were performed on a 486/66 (16 MB RAM) using Release 3.0 of the Hyperchem software. Initial structures were built using the default model-building routine. After a single-point calculations to set the Mullikan charge populations was performed, the structure was minimized with MM+ (Hyperchem's version of MM2) using the partial charge option. The Polak–Ribiere block diagonal algorithm was used for all MM+ and semiempirical minimizations to an RMS gradient of <0.1 kcal/[Å mol]. All semiempirical calculations[6] were unrestricted Hartree–Fock with the wave function calculated to a convergence limit of <0.001.

To construct the energy profiles, the $C_1$′-nicotinamide bond length was increased in steps from the initial length of 1.49–1.52 Å using the restraint function to a final restraint force constant of $10^5$, the value recommended by Hyperchem. Each structure was minimized completely with no restraint other than the reaction coordinate. Values of $\Delta H_f$ for each structure were used to construct energy profiles and locate the approximate energy of the transition state; structures were refined until the criterion of a single negative (imaginary) frequency[7] was obtained for the reaction coordinate using the Vibrational Analysis function. Energies of the oxocarbenium ions were calculated after removal of nicotinamide from the IDC.

## Results

**Experimental.** In the tandem LSIMS spectra of **1a–e**, the most abundant peak is the respective molecular

† Present address: Burroughs-Wellcome Co., 3030 Cornwallis Rd., Research Triangle Park, NC 27709.

® Abstract published in *Advance ACS Abstracts*, May 15, 1994.

(1) Johnson, R. W.; Marshner, T. M.; Oppenheimer, N. J. *J. Am. Chem. Soc.* **1988**, *110*, 2257–2263.

(2) Handlon, A. L.; Oppenheimer, N. J. *J. Org. Chem.* **1991**, *56*, 5009–5010.

(3) Tarnus, C.; Schuber, F. *Bioorg. Chem.* **1987**, *15*, 31–42. Tarnus, C.; Muller, H. M.; Schuber, F. *Ibid.* **1988**, *16*, 38–51.

(4) Schuber, F.; Xu, C.; Oppenheimer, N. J., in preparation.

(5) Sleath, P. R.; Handlon, A. L.; Oppenheimer, N. J. *J. Org. Chem.* **1991**, *56*, 3608–3613.

(6) AM1:Dewar, M. J. S.; Zoebisch, E. G.; Healy, E. F.; Stewart, J. J. P. *J. Am. Chem. Soc.* **1985**, *107*, 3902–3909. PM3:Stewart, J. J. P. *J. Comput. Chem.* **1989**, *10*, 209–220.

(7) McIver, J. W., Jr.; Komornicki, A. *Chem. Phys. Lett.* **1971**, *10*, 303–306.

0022-3263/94/1959-3609$04.50/0 

**Scheme 1**

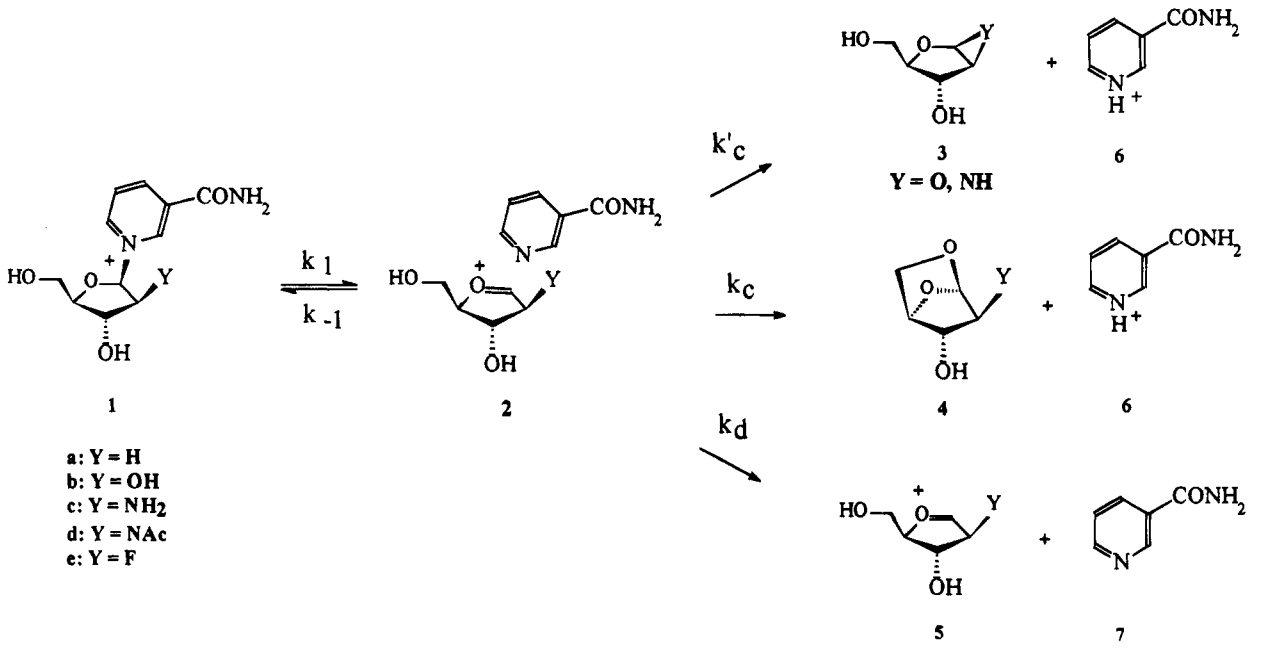


**Table 1. Relative Abundances for the Gas-Phase Dissociation of 2′-Substituted β-Nicotinamide Arabinosides ($M^+$ = 100)**

| Y | Nic-$H^+$ | oxocarbenium ions | log($R^+$/[$R^+$ + $M^+$])[a] |
|---|---|---|---|
| H | 20 | 11 | −0.62 |
| $NH_2$ | 14 | 10 | −0.71 |
| OH | 15 | 4 | −0.80 |
| HNAc | 5(13)[b] | 11(3)[b] | −0.86 |
| F | 12 | 0.8 | −0.95 |

[a] $R^+$ = Nic-$H^+$ + oxocarbenium ion. [b] The numbers in parentheses are the expected values obtained by extrapolation from a plot of log($R^+$/[$R^+$ + $M^+$]) vs the relative abundance of Nic-$H^+$ and oxocarbenium ions.

ion, followed by peaks for protonated nicotinamide (**7**, Nic-$H^+$) and the respective oxocarbenium ion.[8] Data are listed in Table 1. As shown in Scheme 1, proton transfer within an IDC and cyclization leads to Nic-$H^+$ and neutrals. The alternative is dissociation of the IDC to the free oxocarbenium ions **5a−e** and unprotonated nicotinamide ($k_d$). If all these processes occur, the total intermediate **2** formed by the two channels (designated $R^+$) is the sum of Nic-$H^+$ and the respective oxocarbenium ion.

A plot of the log($R^+$/[$R^+$ + $M^+$]) for **1a−e** vs $\sigma_F$ is shown in Figure 1; the $\sigma_F$ value for NAc is not available, but was estimated to be +0.33 by interpolation with the $\sigma_I$ scale.[9] The plot is linear. With the point for 2′-OH included, $r$ = 0.990, and with the point excluded $r$ = 0.999. In either case, $\rho_F$ = −0.75. The Taft correlation implies a correlation with the solution kinetics ($k_w$), and a plot (not shown) of log $k_w$ vs log($R^+$/[$R^+$ + $M^+$]) is linear ($r$ = 0.988) with a slope of −0.25.

**Computational. Methods.** Hyperchem Release 3 was not designed to do explicit transition state modeling; nonetheless, all the methods needed to perform these calculations are in the software, including a modified version of MM2, the full range of semiempirical methods, and a subroutine for diagonalization of the force constants. Two modifications of the standard approach to transition state modeling should be mentioned.

(8) The 2′-azido substrate reported in ref 2 did not give a peak corresponding to the oxocarbenium ion and was not included in this analysis.

(9) Taft, R. W.; Topsom, R. D. *Prog. Phys. Org. Chem.* **1987**, *16*, 2−83.

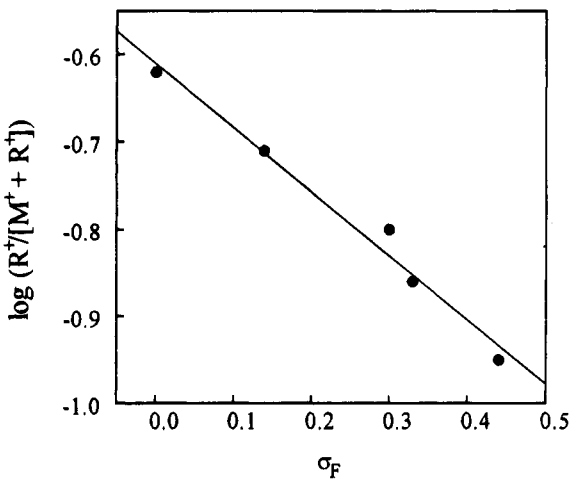


**Figure 1.** Taft plot for the gas-phase dissociation of 2′-substituted β-nicotinamide arabinosides. The $\sigma_F$ value for NAc is not available, but was estimated as described in the text. The plot is linear ($r$ = 0.990) with $\rho_F$ = −0.75. Left to right the points are for Y = H, $NH_2$, OH, NAc, and F.

First, we found that the time needed to do a complete minimization using semiempirical methods could be cut by one-half to two-thirds if the restraint force constant on the reaction coordinate bond was increased in three equal steps from $10^3$ to $10^5$. Values of $\Delta H_f$ obtained with the stepped approach were <±0.1 kcal/mol of the value obtained by setting the force constant to $10^5$ at the outset of the calculation. For instance, increasing the bond in **1c** from 2.0 to 2.2 Å gave a $\Delta H_f$ of 6.65 kcal/mol for the direct approach and a value of 6.62 kcal/mol for the stepped approach. We do not consider these small differences to be significant for these calculations.

Second, the Vibrational Analysis subroutine was designed to generate IR spectra; complete values for the diagonalized force constants but not the values of the eigenvalues in the Hessian are recorded in the output. The normal mode analysis does provide negative (imaginary) frequencies, however, and the graphic display can localize the frequency to the bond involved. In all cases, the single negative frequency found—the first normal mode—corresponded to the reaction coordinate.[10]

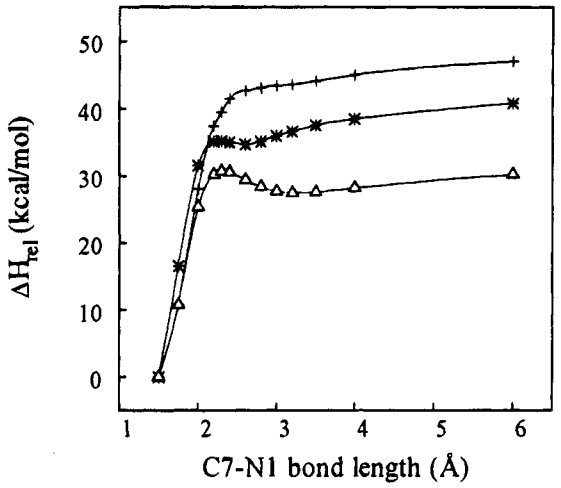


**Figure 2.** PM3 (+), AM1 (*), and MNDO (Δ) energy profiles calculated for benzyl pyridinium using Hyperchem Release 3. The calculated profiles are an exact match for reported profiles (Figure 5 of ref 11).

Because this approach to transition state modeling has not been documented previously, we generated the energy profiles shown in Figure 2 for unsubstituted benzyl pyridinium with the MNDO, AM1, and PM3 methods. Two of the three—AM1 and MNDO—show distinct maxima that meet the criterion of a saddle point on a potential energy surface. As expected, the AM1 and MNDO methods give different energies for the transition state. These plots match exactly those published by Katritzky, Anders, Ford, and colleagues (Figure 5 of ref 11) who used MOPAC and much more sophisticated stopping criteria for minimization than available in Hyperchem.

**Activation Enthalpies.** In earlier calculations of the gas-phase dissociation of β-nicotinamide riboside we used the PM3 methodology in preference to AM1.[12] Katritzky, Anders, Ford, and colleagues,[11] however, found that PM3 failed to provide a distinct transition state for a series of benzyl pyridiniums. For **1a**–**e**, PM3 gave acceptable energy profiles and met the criterion for transition state saddle points, but a plot of $\Delta H^{\ddagger}$ vs $\log(R^+/[R^+ + M^+])$ is badly scattered with a correlation coefficient of 0.60, although a general trend correlating the data is evident.

Therefore, the calculations were repeated using the AM1 method. AM1 values for $\Delta H_f$ for the starting structures, transition states, IDCs, oxocarbenium ions, and related neutral structures are listed in Table 2. Values of $\Delta H^{\ddagger}$ for bond cleavage and dissociation and enthalpies of the various structures relative to the starting structure are listed in Table 3.

There are two apparent anomalies in the energy profiles shown in Figure 3. First, in the profile for the 2′-$NH_2$ compound **1c** there is a drop in energy of 3.9 kcal/mol between 2.6 and 2.8 Å (closed squares, Figure 3). Examination of the structures shows that the nicotinamide ring has rotated about the reaction coordinate and formed a hydrogen bond between the amide carbonyl and the 5′-OH proton, which stabilizes the structure.

Second, the energy profile for the 2′-OH compound **1b** gives an energy for the transition state that is higher than the other values (open up triangles, Figure 3). In a plot of $\log(R^+/[R^+ + M^+])$ vs the AM1-calculated $\Delta H^{\ddagger}$, the points for all substrates except **1b** form a straight line (Figure 4, $r = 0.9999$); the energy for **1b** is too high by 3.9 kcal/mol (open circle, Figure 4). This apparent anomaly can be resolved by examining and comparing the calculating structures for all substrates.

In the ground and transition states and IDCs for **1a** and **1e**, the plane of the nicotinamide ring lies directly along and above the C′1-C′2 bond (Figure 5, *left*). In the NAc compound, however, the nicotinamide is forced by steric repulsion to rotate away from the substituent, and a hydrogen bond forms between the carbonyl of the nicotinamide amide and the 5′-OH proton (Figure 5, *right*); this conformation is retained from the ground to the transition state and into the IDC. In the structures for the 2′-OH substrate **1b**, the ground state resembles the structure for **1a** and **1e** (Figure 6, *left*). As the bond length in **1b** is increased, however, the nicotinamide rotates about the reaction coordinate and a hydrogen bond forms between the carbonyl of the nicotinamide amide and the 5′-OH (Figure 6, *right*). Thus there is a difference in energy between the ground and transition states that is not produced by merely breaking the bond. Normalizing the ground-state energy by adding the 3.9 kcal/mol for formation of this hydrogen bond gives $\Delta H^{\ddagger} = 23.3$ kcal/mol, a value that fits quite nicely on the plot of $\log(R^+/[R^+ + M^+])$ vs $\Delta H^{\ddagger}$ (Figure 4, solid circle).

As the $C_1'$-nicotinamide bond length is increased, the geometry about the reaction center flattens and the charges on both the ring oxygen and $C_1'$ increase to a plateau value in all substrates. The energies and charge distributions in the activated complexes and IDCs fit the description[11] for structures expected to form by heterolytic cleavage of the ribosyl–nicotinamide bond.

For all compounds, the barriers between the IDC and complete dissociation $k_d$, Scheme 1, are lower (10–14.7 kcal/mol) than the barriers for cleavage of the ribosyl–nicotinamide bond (20.7–26 kcal/mol). Moreover, the barriers for the return reaction $k_{-1}$, Scheme 1 (3.3–5.4 kcal/mol) are lower than those for $k_d$. Because the barrier to proton transfer is generally lower than the barrier to complete dissociation,[13] and because the ribosyl zwitterions would be expected to collapse with no barrier,[12] neither of the mechanisms that form neutrals is rate limiting. Therefore, the rate-limiting step is cleavage of the ribosyl–nicotinamide bond.

**Structures of Oxocarbenium Ions and the Site of Protonation of Nicotinamide.** In Schemes 1 and 2, we have drawn the structures of the oxocarbanium ions as ring structures and Nic-$H^+$ as the ring N-protonated species, when in fact we know with certainty only the value of *m/z*. It is possible that the ring structures could open to give O=CHCHYCH(OH)CH(+)$CH_2$OH that by nicotinamide-catalyzed β-elimination could give one (or both) of two enols, O=CHCHYCH(OH)=$CHCH_2$OH or O=CHCHYCHOHCH=CHOH.[14] When the cyclic form of the oxocarbenium ions are opened and minimized in MM+, linear carbenium ions result. When these structures are minimized in AM1, however, they return through rather convoluted pathways back to the cyclic oxocarbenium ion structures (in the $[=OC]^+$ canonical form). Computationally, at least, the cyclic oxocarbenium structures are more stable than the open-chain forms of the cations. This is not surprising because oxygens α to

(10) Thomas Slee of Hypercube confirms that this use of the Vibrational Analysis subroutine is valid for these calculations.
(11) Katritzky, A. R.; Malhotra, N.; Ford, G. P.; Anders, E.; Tropsch, J. G. *J. Org. Chem.* **1991**, *56*, 5039–5044.
(12) Schröder, S.; Buckley, N.; Oppenheimer, N. J.; Kollman, P. A. *J. Am. Chem. Soc.* **1992**, *114*, 8231–8238.
(13) Bowen, R. D. *Acc. Chem. Res.* **1991**, *24*, 364–371.
(14) We thank John Bartmess for pointing out this possibility.

**Table 2. Absolute AM1 Enthalpies of Formation ($\Delta H_f$) for the Gas-Phase Dissociation of 2′-Substituted β-Nicotinamide Arabinosides[a]**

| substituent | starting structure | transition state | ion–dipole complex | oxocarbenium ion | bicyclic structure | other structures[b] |
|---|---|---|---|---|---|---|
| H | 10.7 | 31.4 | 28.2 | 44.0 | −119.3 | – |
| $NH_2$ | 14.0 | 36.3 | 33.1 (29.2)[d] | 49.6 | −117.9 | −100.8 |
| OH | −31.2[c] | −7.90 | −12.7 | 7.3 | −160.9 | −142.2 |
| NAc | −23.5 | 0.70 | −4.7 | 15.6 | −155.4 | −13.3 |
| F | −32.8 | −6.80 | −9.6 | 10.9 | −163.5 | – |

[a] All energies in kcal/mol. $\Delta H_f$ nicotinamide = −5.8. $\Delta H_f$ Nic-N−$H^+$ = 150.1. $\Delta H_f$ Nic-$NH_2$C=O−$H^+$ = 154.4. [b] $NH_2$, β-1′,2′-aziridine; OH, β-1′,2′-epoxide; NAc, β-1′,2′-acylium ion. [c] Corrected by adding the energy of formation of a hydrogen bond between the nicotinamide amide carbonyl and the 5′-OH on going to the transition state. [d] Value in parentheses is after formation of a hydrogen bond between the nicotinamide amide carbonyl and the 5′-OH between 2.6 and 2.8 Å.

**Table 3. Relative AM1 Enthalpies of Formation ($\Delta H_f$) and Activation ($\Delta H^{\ddagger}$) for the Gas-Phase Dissociation of 2′-Substituted β-Nicotinamide Arabinosides[a]**

| substituent | ion–dipole complex | oxocarbenium ion | bicyclic structure | other structures[b] | dissociation[c] | $\Delta H^{\ddagger}$ $k_1$ | $\Delta H^{\ddagger}$ $k_{-1}$ | $\Delta H^{\ddagger}$ dissociation |
|---|---|---|---|---|---|---|---|---|
| H | 17.4 | 33.3 | 20.1 | – | 27.5 | 20.7 | 3.3 | 10.1 |
| $NH_2$ | 15.2 (19.1)[d] | 35.6 | 18.2 | 35.3 | 29.8 | 22.3 | 7.1 (3.2) | 14.6 |
| OH | 18.5 | 38.5 | 20.4 | 39.1 | 32.7 | 23.3 | 4.8 | 14.2 |
| NAc | 18.8 | 39.1 | 18.2 | 4.6 | 33.3 | 24.2 | 5.4 | 14.5 |
| F | 32.2 | 43.7 | 19.4 | – | 37.9 | 26.0 | 2.8 | 14.7 |

[a] All energies in kcal/mol relative to respective starting structure, except for the $\Delta H^{\ddagger}$ for $k_{-1}$ and dissociation, which are relative to the respective ion–dipole complexes. [b] $NH_2$, β−1′,2′-aziridine; OH, β-1′,2′-epoxide; NAc, β-1′,2′-acylium ion. [c] $\Delta H_f$ [oxocarbenium ion] + $\Delta H_f$ [nicotinamide]. [d] Value in parenthesis is after formation of a hydrogen bond between the nicotinamide amide carbonyl and the 5′-OH between 2.6 and 2.8 Å.

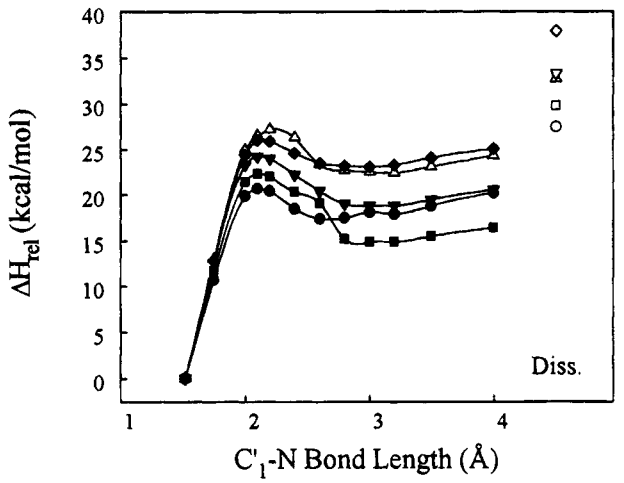


**Figure 3.** AM1 energy profiles for gas-phase dissociation of **1a–e**. Y = H (●); OH (△); $NH_2$ (■); NAc (▼); F (◆). The difference between $\Delta H_f$ for the starting structure and the maximum value is $\Delta H^{\ddagger}$. Energy values obtained from these plots are listed in Tables 2 and 3.

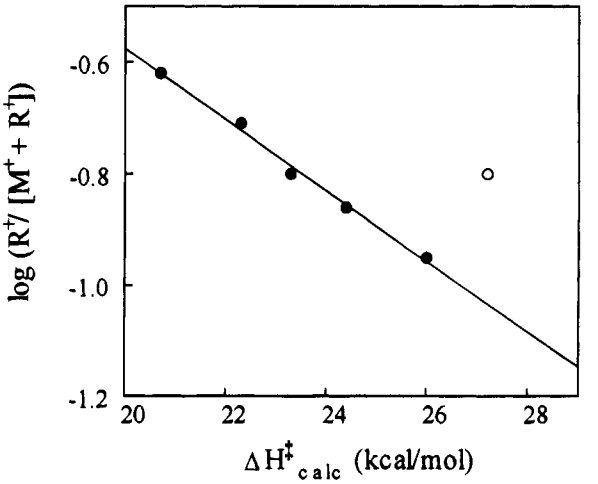


**Figure 4.** Plot of the experimentally determined log($R^+$/[$R^+$ + $M^+$]) vs the AM1-calculated values of $\Delta H^{\ddagger}$ for gas-phase dissociation of **1a–e** ($r$ = 0.998). The open circle is the value for the 2′-OH compound **1b** before normalization as described in the text. Left to right the points are for Y = H, $NH_2$, OH, NAc, and F.

cationic centers confer an enormous amount of stabilization energy, even in ring structures.[12]

There are two sites of protonation on the nicotinamide, the ring nitrogen and the amide carbonyl. The AM1 $\Delta H_f$ for the two protonated species show that the ring N-protonated species is 4.3 kcal/mol more stable than the O-protonated form (150.1 vs 154.4 kcal/mol, respectively). As discussed above, in several of the IDCs there is a hydrogen bond between the amide carbonyl and the 5′-OH proton, which could lead to concerted removal of a proton during dissociation (for **1b,d**) or favor O-protonation within the IDC (**1b–d**). We argue below that concerted proton abstraction in **1d** is inconsistent with the experimental results. Because of the regular, monotonic change in Nic-$H^+$ along the series, which includes two structures in which there is no apparent hydrogen bond between the amide carbonyl and the 5′-OH proton (**1a,e**), we suspect that the site of protonation in Nic-$H^+$ is relatively unimportant; the important point is that proton transfer occurs at all. It is also highly probable that *all* of the hydrogen-bonded structures are an artifact of the AM1 method; no hydrogen-bonded structures were seen in the PM3 structures.

**Correlation with Solution Activation Values.** There is a crude correlation ($r$ = 0.919, not shown) between $\Delta H^{\ddagger}$ for the solution and gas-phase dissociations; Handlon[15] found a similar crude correlation between the rates and enthalpies for the solution reaction. Assuming that $-T\Delta S^{\ddagger}$ is constant for this series in the gas phase, a plot of the solution $\Delta G^{\ddagger}$ vs the gas phase $\Delta H^{\ddagger}$ should represent a direct linear free energy relation (LFER); this plot (Figure 7) is linear ($r$ = 0.994, slope = 0.94) and shows that the relative effects of substituents on the dissociation reaction are independent of the phase. The absolute correlation,

(15) Handlon, A. L.; Oppenheimer, N. J., in preparation.

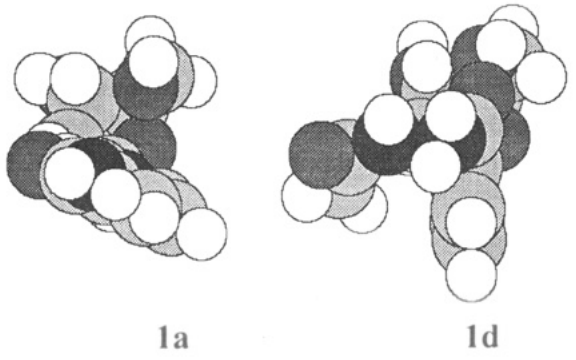


**Figure 5.** CPK rendering of the ground states for the 2′-H (**1a**) and 2′-NAc (**1d**) compounds. View is along the plane of the nicotinamide into the plane of the ribose. There is no hydrogen bond between the amide carbonyl and the 5′-OH for **1a** but this bond exists for **1d**. Shadings: darkest, nitrogen; medium, oxygen; lightest, carbon; white, hydrogen.

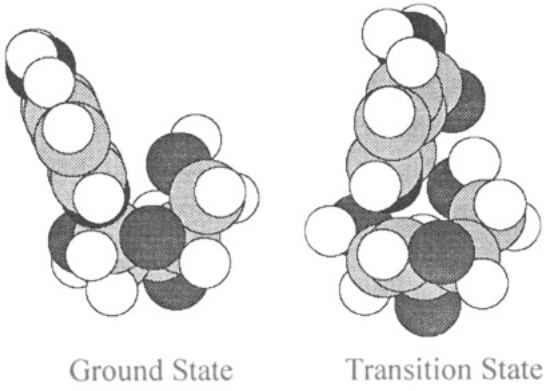


**Figure 6.** CPK renderings for the ground state (*left*) and transition state (*right*) for **1b** that show formation of a hydrogen bond between the amide carbonyl and the 5′-Oh proton during cleavage of the ribosyl−nicotinamide bond. Shadings are the same as in Figure 5.

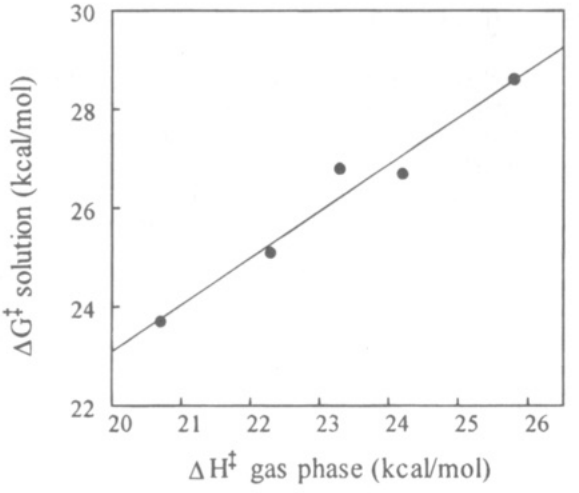


**Figure 7.** Plot of $\Delta G^{\ddagger}$ for the hydrolysis of **1a**−**e** (ref 19) vs the AM1-calculated values of $\Delta H^{\ddagger}$ ($r$ = 0.994). Left to right the points are for Y = H, $NH_2$, OH, NAc, and F.

of course, would depend on the entropies for the gas phase, which are not available.

## Discussion

In comprehensive reviews, Morton[16,17] has presented compelling evidence that radical cations and some even-electron ions such as protonated ethers[18] dissociate in the gas phase through IDCs, which are equivalent to a contact ion pair in the Winstein scheme.[19] Heterolysis ($RX^+ \rightarrow R^+ + X^\circ$) is favored over homolysis ($RX^+ \rightarrow R\bullet\ X\bullet^+$) if the charge remains on the fragment that did not contain it initially. If $R^+$ is a stable carbenium ion, and X is an electronegative, polarizable group, as is the case with our substrates, heterolysis should be favored. Recently McAdoo and Morton[17] pointed out that heterolytic cleavage favors formation of an IDC rather than simple dissociation of the fragments. Depending on the chemistry, proton transfers tend to take place more efficiently within IDCs than between members of a dissociative fragment pair.

In some ribosyl systems, concerted proton transfer during dissociation is possible. McCloskey and co-workers[20] have reported correlations between the solution and gas-phase dissociation of 7- and 9-β-D-ribofuranosylpurines in chemical ionization mass spectra (CIMS). The relative abundances of these species ($BH_2^+/M^+$) correlate with the rate constants for hydrolysis (plot not shown; $r$ = 0.89).[21] On the basis of isotopic labeling experiments, these workers suggested that a prominent rearrangement of protonated purine nucleosides in CIMS occurs by heterolysis with concerted abstraction of a proton from an available sugar hydroxyl by a second heteroatom on the purine. The ribosyl zwitterion collapses to a neutral, bicyclic product. We performed transition-state modeling (PM3) on deoxyadenosine and found that there is a hydrogen bond between the purine $N_3$ and the 5′-OH proton during the entire course of glycosyl bond cleavage, which is consistent with a concerted mechanism of proton abstraction. No IDC would be formed during this bond cleavage.

Katritzky *et al.* have studied the gas-phase dissociation of pyridinium substrates[22] and have reported the results of semiempirical calculations (MNDO, AM1, and PM3) for dissociation of pyridinium substrates in which the structures of both the putative carbenium ions and pyridine leaving groups were varied.[11] Their results are consistent with dissociation to IDCs in the gas phase.

We have obtained tandem LSIMS spectra for a series of 4-substituted benzyl substrates with different pyridine leaving groups and of the corresponding substituted benzyl dimethylsulfoniums.[23] While results for the dimethylsulfonium compounds give an excellent Hammett plot [vs $\sigma^+$], Hammett plots for benzyl substrates with nicotinamide, pyridine, and 3-chloro- and 3-cyanopyridine leaving groups show a drastic downward break between 4-chloro- and 4-nitrobenzyl compounds. The MNDO-calculated energy profiles for the sulfonium series are well-behaved, reaction coordinate bond lengths at the transition state follow the Hammond Postulate, energies are consistent with an IDC intermediate, and the calculated values of

(16) Morton, T. H. *Tetrahedron* **1982**, *38*, 3195−3243.

(17) McAdoo, D. J.; Morton, T. H. *Acc. Chem. Res.* **1993**, *26*, 295−302.

(18) Kondrat, R. W.; Morton, T. H. *J. Org. Chem.* **1991**, *56*, 952−957.

(19) Carpenter, B. K. *Determination of Organic Reaction Mechanisms*; Wiley-Interscience: New York, 1984; pp 40−49, gives an excellent brief review of the Winstein ion-pair scheme.

(20) (a) McCloskey, J. A.; Futrell, J. H.; Elwood, T. A.; Schram, K. H.; Panzica, R. P.; Townsend, L. B. *J. Am. Chem. Soc.* **1973**, *95*, 5762−5764. (b) Wilson, M. S.; McCloskey, J. A. *J. Am. Chem. Soc.* **1975**, *97*, 3436−3444. (c) McCloskey, J. A. *Acc. Chem. Res.* **1991**, *24*, 81−87.

(21) We determined these $r$ values from plots of log $k_{hydrolysis}$ vs log-[$BH_2^+/M^+$] reported in ref 20a. If nebularine is included in the analysis for the 7-substituted compounds, $r$ = 0.69.

(22) Katritzky, A. R.; Watson, C. H.; Dega-Szafran, Z.; Eyler, J. R. *J. Am. Chem. Soc.* **1990**, *112*, 2471−2478.

(23) Buckley, N.; Maltby, D.; Burlingame, A. L.; Oppenheimer, N. J., unpublished results.

$\Delta H^{\ddagger}$ correlate well with the gas-phase experimental results. We will report these results elsewhere.

Thus there are gas-phase results for precursors that give ribosyl oxocarbenium ions and for pyridinium and other charged substrates that are consistent with formation of an IDC as an intermediate in gas-phase dissociation. Despite the precedents, however, we are not sanguine about assigning a mechanism for the dissociation of our compounds. We believe that a close analysis of our data for the NAc derivative **1d** shows the intermediacy of an IDC and that the existence of a series of LFERs that correlate all the data strongly suggests that the entire series of compounds dissociates by the same mechanism. The computational results are consistent with our proposed mechanism.

**Mechanism of Gas-Phase Dissociation.** The most straightforward gas-phase mechanism is direct dissociation to the oxocarbenium ion and neutral nicotinamide. The presence of Nic-H$^+$ rules out this mechanism, unless there is concerted proton transfer during dissociation. Based on the AM1 structures, this could occur only for the NAc compound **1d** because of the constant presence of a hydrogen bond between the amide carbonyl and the 5′-OH. If this occurred, however, the amount of Nic-H$^+$ would be *greater than expected* relative to the correlation with the other compounds; the finding that the relative abundance of Nic-H$^+$ is *much less than expected* rules out concerted dissociation and proton removal in the best case. As discussed above, however, the PM3 structures did not contain similar hydrogen bonds in either the starting, transition state, or IDC structures; the hydrogen-bonded structures may be an artifact of the AM1 method.

The relative abundance of Nic-H$^+$ down the series 2′-H (most-stable oxocarbenium ion) to 2′-F (least-stable oxocarbenium ion) changes by only a factor of 1.75, while the relative abundance of the oxocarbenium ions changes by a factor of 17 (Table 1). Thus, according to the mechanism in Scheme 1, $k_{-1}$ increases and $k_1$ and $k_d$ decrease down the series, while $k_c$ and/or $k_c'$ remain essentially constant as expected for the relative stabilities of the IDCs and the oxocarbenium ions. These trends, while crude, are seen in the calculated enthalpies (Table 3).

The presence of Nic-H$^+$ suggests that proton transfer occurs after the rate-limiting step. Partitioning of an IDC **2** between neutral and charged species can occur by three processes (Scheme 1). Within the IDC, which should be a series of local minima of similar energy, nicotinamide can abstract a proton from the 5′-OH in **1a**–**e** and/or from the 2′-OH or 2′-NH$_2$ in **1b** and **1c** to give zwitterions that can collapse to neutrals. In all substrates when the 5′-OH proton is removed from the respective cation or IDC and minimized in AM1, the zwitterion collapses to the bicyclic structure **4**. The calculated $\Delta H_f$ for all bicyclic structures are within a narrow range (18.2–20.4 kcal/mol relative to the starting structure, Table 3).

For the 2′-OH and 2′-NH$_2$ substituents in **1b**,**c**, there are two possible mechanisms of collapse for the $k'_c$ pathway: either initial abstraction of the proton with collapse of the respective zwitterion to a neutral, or direct cyclization to give the protonated aziridine **3c** or epoxide **3b**, from which the proton could be removed. The respective zwitterionic structures immediately collapse to the aziridine or epoxide on AM1 minimization. In contrast, AM1 minimization of the protonated aziridine or epoxide leads directly back to the cation, which eliminates this mechanism. In fact, collapse to either the aziridine or epoxide may not be energetically favorable. The values for the respective species listed in Table 3 show that the bicyclic structures **4b**,**c** are much more stable than either the aziridine **3c** ($\Delta H_f$ = 35.3 kcal/mol) or the epoxide **3b** ($\Delta H_f$ = 39.1 kcal/mol). The stability of ca. 15 kcal/mol of the bicyclic structures is the result of relief of ring strain relative to the cation. Formation of the neutral bicyclic structure relieves the strain about the reaction center, while formation of either the aziridine or expoxide retains the essentially flat geometry about the reaction center and introduces the additional strain of a three-membered ring. Thus the computational results suggest that proton abstraction and cyclization to **4a**–**e** should be an energetically favored processes, which is borne out by the relative abundances for Nic-H$^+$ and oxocarbenium ions (Table 1). In general, separation of the IDC into a cation and a neutral species is a higher energy process than proton abstraction.[13]

**Scheme 2**

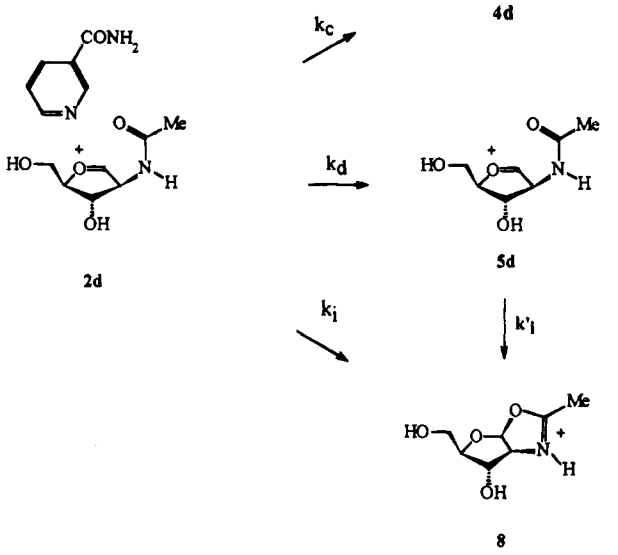


While the total relative abundance of cationic species for the NAc derivative **1d** is within the expected range, the relative abundances of Nic-H$^+$ and **5d**, 5 and 11, respectively, are significantly different than the expected values of 13 and 3 obtained by extrapolation of the relative abundances of the respective species with the totals (not shown). While these data are consistent with an anchimeric assistance mechanism, this process cannot occur in the $\beta$-arabino configuration in which the NAc and the leaving group are *cis*. Solvolysis of α-nicotinamide 2′-NAc arabinoside and $\beta$-nicotinamide NAc riboside, in which the NAc group is *trans* to the leaving group, is anchimerically assisted. In solution this intermediate is sufficiently stable that both the *trans* ara and ribo configurations of **8** have been observed by $^1$H-NMR during hydrolysis.[2,15] The two substrates with the NAc group *cis* to the leaving group hydrolyze with rate constants that correlate with $\sigma_I$.

Of the several possible cyclization pathways (Scheme 2), only one decreases Nic-H$^+$ and increases the abundance of cations with *m/z* 174 (**5d** and **8**). A reasonable assumption would be that nicotinamide is forced to depart because of steric repulsion by the NAc group, although the bulk of substituents did not affect the kinetics of hydrolysis.[2,15] The NAc group in **1d** is polarized and in the IDC can swing into a position to collapse to **8**. When this structure is formed manually and minimized in AM1, the acylium ion **8** forms (Figure 8). In fact, the energies listed in Table 3 show that the acylium ion is more stable than the bicyclic structure ($\Delta H_f$ of 4.6 and 18.2, respectively, relative to the starting structure). Thus, competi-

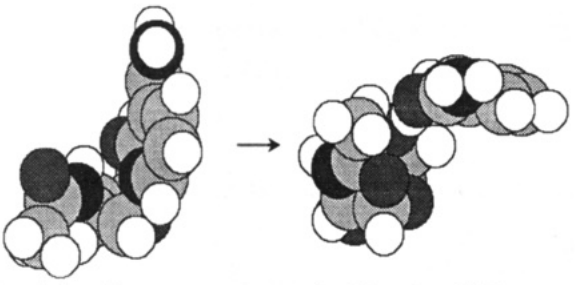


**Figure 8.** CPK rendering of the change in structure between the transition state and cyclization to the acylium ion within the IDC for **1d** (Scheme 2). The nicotinamide ring has been forced up and away from the transition state position. Shadings are the same as for Figure 5.

tion of NAc collapse with proton removal and cyclization within the IDC ($k_i$) would lower Nic-H$^+$ and give **8**, which is the effect observed (Table 1). We believe this interpretation is consistent with an IDC in the gas phase.

**Substituent Effects/LFERs.** Bagno and Scorrano[24] have suggested recently that substituent effects are better differentiated in solution than in the gas phase despite the well-known solvent attenuation (substantially lower values of $\Delta G^\circ$ in solution) and that $\varrho$ values for gas-phase reactions should be clustered about unity, provided the LFERs are constructed with data for substituent effects determined in the same system in the two phases. Both sets of substituent constants used to analyze our data were determined directly from either gas-phase[9] ($\sigma_F$) or solution[25] ($\sigma_I$, 50% v/v EtOH/water) ionization of 4-substituted bicyclo[2.2.2]octane-1-carboxylic acids. Despite the different phases, the values of $\sigma$ are essentially the same in both scales. (Bagno and Scorrano did not define a new $\sigma$ scale in their work, but based their correlations on $\delta_x\Delta G^\circ$ values for ionization of aromatic systems such as phenols and aniliniums.)

The Taft plot of $\log(R^+/[R^+ + M^+])$ vs $\sigma_F$ is shown in Figure 1. The value of $\varrho_F$ of $-0.75$ is substantially less than the $\varrho_I$ of $-6.7$ for the solution reaction.[2] In solution, the $k_{rel}$ for **1a** and **1e**, the extremes of the series, is 3500; in the gas phase, $k_{rel}$ is 2.5. Thus the difference we find in the kinetic $\varrho$ values is similar to that found by Bagno and Scorrano for proton transfer equilibrium $\varrho$ values; the difference is related to the relative dissociation of the substrates and not to the substituent scales used. To our knowledge, this is the first kinetic correlation that shows this effect.

The correlation with substituent constants in each phase implies a correlation between gas-phase and solution dissociation, and a plot of $\log(R^+/[R^+ + M^+])$ vs $\log k_w$ for hydrolysis of the substrates[2] (not shown) is linear ($r = 0.988$). A more direct free energy correlation is shown in Figure 7, which is a plot of $\Delta G^\ddagger$ for the solution hydrolysis vs $\Delta H^\ddagger$ calculated for gas-phase dissociation. This correlation assumes that for a group of substrates with very similar structures, the value of $-T\Delta S^\ddagger$ in the gas phase is relatively constant and is dominated by the entropy for dissociation and translation; vibrational and rotational entropies should be small and of comparable magnitude across the series.

**Mechanisms in the Two Phases.** The existence of a good correlation does *not* mean that we can infer the *mechanisms* in solution and the gas phase are the same. For direct dissociation, the mechanisms in the two phases would be the same. The IDC mechanisms would not be precisely the same in the two phases because there can be no intermediate equivalent to a solvent-separated IDC in the gas phase. Substituents would affect the stabilities of both free oxocarbenium ions and IDCs in the same way, but to different extents. Linearity of LFERs over the entire range of substituents implies a constant mechanism, but this is not diagnostic of what the mechanism is. While the sign of $\varrho$ values is diagnostic of the charge that develops in the transition state relative to the ground state, the absolute values of $\varrho$ can span large ranges for a single mechanism that occurs in substrates of greatly different structure. Thus other evidence is needed to choose among alternative mechanisms.

Handlon[15] found that the presence of up to 2 M nicotinamide did not greatly affect the value of $k_{obsd}$ for hydrolysis of **1a**. The hallmark of an $S_N1$ mechanism is common leaving group suppression; the lack of this effect is indicative of an IDC mechanism, but cannot be used to distinguish between a contact or a solvent-separated pair as kinetically competent intermediates.[19] Ta-Shma and Oppenheimer[26] have evidence from selectivity data in aqueous trifluoroethanol mixtures that the solvolysis of NAD$^+$ occurs through an IDC mechanism, with the IDC trapped at the solvent-separated stage.

Thus both the solution and gas-phase reactions occur through a mechanism that has an IDC intermediate. It is probable, however, that the rate-limiting step is different in the two phases. In solution it is interception of the solvent-separated IDC by solvent or nucleophile. As discussed above, the barrier to separation of the components of the IDC in the gas phase is low. In all substrates, the barrier to complete dissociation relative to the energy of the IDC is less than $\Delta H^\ddagger$ for bond cleavage. Thus in the gas phase the rate-limiting step is formation of the intermediate and not its dissociation. The existence of LFERs that correlate the solution and gas-phase energies must then reflect the *relative* effect of the substituents on the kinetics in the two phases, but the existence of an LFER clearly does not indicate that the mechanisms are strictly the same.

**Acknowledgment.** Supported in part by NIH Grant GM-22982 (N.J.O.), a Biotechnology Grant from the State of California (N.J.O., N.B.), and a Research Award from the UCSF Graduate Division (N.B.). A. L. H. was supported by an NIH Training Grant. Funds for the purchase and support of the tandem spectrometer in the UCSF Mass Spectrometry Facility (A.L. Burlingame, Director) were provided by a grant from the Division of Research Resources (RR 01614) of the NIH and a grant from the NSF (DIR 8700766). We thank Dr. John Bartmess (University of Tennessee) for helpful and insightful correspondence, Randy Radmer, Jim Caldwell, and Peter Kollman (UCSF) and Dave Ferguson (University of Minnesota) for helpful discussions concerning semiempirical calculations and our use of Hyperchem for transition-state modeling, and Dr. Tom Slee (Hypercube, Toronto, Ont.) for conformation of our use of Hyperchem subroutines for the calculations reported here.

(24) Bagno, A.; Scorrano, G. *J. Chem. Soc. Perkin Trans. 2* **1991**, 1601–1606.
(25) Charton, M. *J. Org. Chem.* **1964**, *29*, 1222–1227.
(26) Ta-Shma, R.; Oppenheimer, N. J., in preparation.